Available online at www.sciencedirect.com
SCIENCE DIRECT®
Journal of Organometallic Chemistry 681 (2003) 237–249
Journal of Organometallic Chemistry
www.elsevier.com/locate/jorganchem

Synthesis, structures and reactivity of bis(diphenylphosphino)-methane (dppm)-substituted selenido osmium carbonyl clusters

Shariff E. Kabir, *[a], Salina Pervin[a], Nitai C. Sarker[a], Afroza Yesmin[a], Ayesha Sharmin[a], Tasneem A. Siddiquee[b], Daniel T. Haworth[b], Dennis W. Bennett[b,*], K.M. Abdul Malik[c]

[a] Department of Chemistry, Jahangirnagar University, Savar, Dhaka 1342, Bangladesh
[b] Department of Chemistry, University of Wisconsin-Milwaukee, Milwaukee, WI 53211, USA
[c] Department of Chemistry, Cardiff University, P.O. Box 912, Park Place, Cardiff CF10, UK

Received 17 January 2003; received in revised form 30 May 2003; accepted 16 June 2003

Abstract

The unsaturated cluster $[(\mu\text{-H})Os_3(CO)_8\{Ph_2PCH_2P(Ph)C_6H_4\}]$ (**2**) reacts with elemental selenium at 110 °C to give two triosmium clusters $[Os_3(CO)_7(\mu_3\text{-Se})_2(\mu\text{-dppm})]$ (**3**), $[Os_3(CO)_7(\mu_3\text{-CO})(\mu_3\text{-Se})(\mu\text{-dppm})]$ (**4**) and the tetraosmium cubane-like cage cluster $[Os_4(CO)_{10}(\mu_3\text{-Se})_4(\mu\text{-dppm})]$ (**5**) in 20, 47 and 5% yields, respectively. Treatment of the labile cluster $[Os_3(CO)_{10}(MeCN)_2]$ with dppmSe at ambient temperature gives the dinuclear compound $[Os_2(CO)_6(\mu\text{-Se})(\mu\text{-dppm})]$ (**6**) along with **3** and **4** in 13, 24 and 4% yields, respectively, while with $dppmSe_2$ at 80 °C it yields **3** and **5** in 27 and 7% yields, respectively, by oxidative transfer of selenium atoms to the metal center. The reaction of **3** with Me_3NO at 80 °C leads to loss of 1 mol of CO and formation of the condensation derivative $[Os_6(CO)_{12}(\mu_3\text{-Se})_4(\mu\text{-dppm})_2]$ (**7**), containing a central 64-electron butterfly core, in 75% yield. Compound **7** reacts with CO at 98 °C to regenerate **4** by cleavage of the three unsupported metal–metal bonds. In the disubstituted square-pyramidal selenido cluster, **3**, the dppm ligand bridges two bonded osmium atoms whereas in **7** both the dppm ligands bridge the open osmium–osmium edges. Treatment of **3** with PPh_3 in the presence of Me_3NO at room temperature gives the phosphine-substituted compound $[Os_3(CO)_6(\mu_3\text{-Se})_2(\mu\text{-dppm})(PPh_3)]$ (**8**) and the dimer **6** in 26 and 20% yields, respectively. The structure of **8** is comparable with that of **3** from which it is derived by replacing one equatorial carbonyl group with the PPh_3 ligand. The molecular structures of the complexes **3**, **4**, **6**, **7** and **8** have been fully elucidated by single-crystal X-ray diffraction studies.

Keywords: Selenium ligands; Triosmium clusters; Tetraosmium clusters; Crystal structure

1. Introduction

Transition metal clusters containing chalcogenido ligands have important chemical and structural significance, since they can be regarded as discrete molecular models of extended inorganic solids with novel electronic, magnetic and optical properties and can be used in cluster growth reactions [1,2]. Furthermore, the combination of chalcogen elements and transition metals often plays a key role in stabilizing the cluster bonding network and frequently introduces novel structural and reactivity features [2,3]. There are numerous examples of the synthesis and reactivity of simple trinuclear clusters of iron, ruthenium and osmium and their monophosphine derivatives containing capping chalcogenido ligands [4–6]. In contrast, there are few reports concerning the synthesis and reactivity of diphosphine-substit uted chalcogenido trimetallic carbonyl clusters. A simple one-step synthetic methodology for the monophosphine and diphosphine-substituted selenido trimetallic compounds of iron and ruthenium has been developed by exploiting the lability of the P=E bond of the tertiary phosphine chalcogenides, which allows for the facile formation of phosphine-substituted chalco-

* Corresponding authors. Tel.: +1-414-229-5276; fax: +1-414-229-5530.
E-mail addresses: skabir_ju@yahoo.com (S.E. Kabir), dwbent@uwm.edu (D.W. Bennett).

0022-328X/03/$ - see front matter © 2003 Elsevier B.V. All rights reserved.
doi:10.1016/S0022-328X(03)00627-2

genido clusters through oxidative transfer of chalcogen atoms to low valent metal centers [5–7]. Despite the synthetic potential of the diphosphine selenides, their reactions with osmium carbonyl clusters have not thus far been explored. The simple triosmium selenido compounds $[Os_3(CO)_9(\mu_3\text{-}Se)_2]$, obtained from the thermolysis of $[Os_3(CO)_{10}(\mu\text{-}SePh)_2]$ and $[(\mu\text{-}H)_2Os_3(CO)_9(\mu_3\text{-}Se)]$, synthesized from the reaction of $[Os_3(CO)_{12}]$ with elemental selenium at 128 °C were described in the literature a number of years ago [4d]. Other selenido osmium carbonyl cluster compounds, such as $Os_4(CO)_{12}(\mu_3\text{-}Se)_2$ have been prepared by the reaction of substituted osmium carbonyl cluster compounds with PhSeH, followed by the thermal elimination of benzene [4e]. However, to our knowledge, little is known about the phosphine and diphosphine-substituted derivatives of these selenido osmium carbonyl cluster compounds.

The chemistry of the bridging dppm triosmium cluster $[Os_3(CO)_{10}(\mu\text{-dppm})]$ (**1**) and its orthometallated derivative $[(\mu\text{-}H)Os_3(CO)_8\{Ph_2PCH_2P(Ph)C_6H_4\}]$ (**2**) has been studied by several groups [8–19] and continues to be the focus of considerable attention. The interest in these complexes is due not only to the special ability of the diphosphine ligand to maintain the structural integrity of the metal cluster framework during chemical reactions, but also because of the unsaturated nature of **2**, which allows it to react with various small inorganic and organic molecules such as CO [9], H_2 [10], PPh_3 [11], $P(OMe)_3$ [11], PPh_2H [12], PhC≡CPh [13], $[Au(PPh_3)]PF_6$ [14], HBF_4 [14], $[Sn\{CH(SiMe_3)_2\}_2]$ [15], EtSH [16], PhSH [16], pySH [17], pymSH [17], $HSCH_2CH_2SH$ [18], $HSCH_2CH_2CH_2SH$ [18] and CH_2N_2 [19] to give many interesting and potentially useful compounds. We have recently reported [20] the synthesis and structural characterization of $[Os_3(CO)_7(\mu_3\text{-}S)_2(\mu\text{-dppm})]$ as two separable isomeric forms from the reaction of $[Os_3(CO)_{10}(\mu\text{-dppm})]$ with tetramethylthiourea at 110 °C.

We report here the results of our investigation on the reactivity of the unsaturated triosmium cluster **2** with elemental selenium and the labile triosmium cluster $[Os_3(CO)_{10}(MeCN)_2]$ with dppmSe and $dppmSe_2$. Of particular interest is the establishment of the viability of the synthesis of triply bridging selenido triosmium clusters containing the bridging dppm ligand and the exploration of their derivative chemistry. These compounds are believed to be the first examples of osmium clusters containing bridging dppm and selenium ligands to be structurally characterized.

2. Experimental

All reactions were routinely performed under a nitrogen atmosphere using standard Schlenk techniques unless specified otherwise. Reagent grade solvents were dried and distilled prior to use by standard methods. Black selenium, triphenylphosphine and dppm were purchased from Aldrich and used as received. Infrared spectra were recorded on a Shimadzu FTIR 8101 spectrophotometer. ^{1}H- and $^{31}P\{^1H\}$-NMR spectra were recorded on a Bruker DPX 400 spectrometer. The elemental analysis was performed at the Microanalytical Laboratory of the Chemistry Department at the University College London. The compounds $[(\mu\text{-}H)Os_3(CO)_8\{Ph_2PCH_2P(Ph)C_6H_4\}]$ [14] (**2**), $[Os_3(CO)_{10}(MeCN)_2]$ [21], dppmSe [22] and $dppmSe_2$ [22] were prepared according to literature procedures.

2.1. Reaction of $[(\mu\text{-}H)Os_3(CO)_8\{Ph_2PCH_2P(Ph)C_6H_4\}]$ (2) with elemental selenium

To a toluene solution (20 ml) of **2** (0.102 g, 0.087 mmol) was added elemental black selenium (0.015 g, 0.190 mmol) and the reaction mixture was heated to reflux for 1.5 h during which time analytical TLC indicated complete consumption of **2**. The solvent was removed under reduced pressure and the residue was chromatographed by TLC on silica gel. Elution with hexane/CH_2Cl_2 (3:1, v/v) produced three bands. The faster-moving band afforded $[Os_3(CO)_7(\mu_3\text{-}Se)_2(\mu\text{-dppm})]$ (**3**) (0.023 g, 20%) as orange crystals after recrystallization from hexane/CH_2Cl_2 at 20 °C. IR (νCO, CH_2Cl_2): 2067 vs, 2000 vs, 1985 sh, 1944 s cm^{-1}; ^{1}H-NMR ($CDCl_3$): δ 7.80 (m, 2H), 7.41 (m, 13H), 7.13 (m, 1H), 7.05 (m, 2H), 6.74 (m, 2H), 5.93 (m, 1H), 3.93 (m, 1H) ppm; $^{31}P\{^1H\}$-NMR ($CDCl_3$): δ −7.6 (d, $J = 92.4$ Hz), −23.1 (d, $J = 92.4$ Hz) ppm; mass spectrum: m/z 1310. Anal. Calc. for $C_{32}H_{22}O_7Os_3P_2Se_2$: C, 29.36; H, 1.70; P, 4.73. Found: C, 29.48; H, 1.82; P, 4.91%.

The second band gave $[Os_3(CO)_7(\mu_3\text{-}CO)(\mu_3\text{-}Se)(\mu\text{-dppm})]$ (**4**)·CH_2Cl_2 (0.055 g, 47%) as yellow crystals from hexane/CH_2Cl_2 at −4 °C by slow evaporation of the solvents. IR (νCO, CH_2Cl_2): 2071 s, 2016 vs, 1995 s, 1960 m cm^{-1}; IR (νCO, KBr): 1734 s cm^{-1}; ^{1}H-NMR ($CDCl_3$): δ 7.63 (m, 4H), 7.41 (m, 4H), 7.26 (m, 4H), 7.18 (m, 4H), 5.27 (m, 1H), 3.41 (m, 1H) ppm; $^{31}P\{^1H\}$-NMR ($CDCl_3$): δ −21.2(s) ppm; mass spectrum: m/z 1258. Anal. Calc. for $C_{34}H_{24}Cl_2O_8Os_3P_2Se$: C, 30.41; H, 1.80; P, 4.61. Found: C, 30.58; H, 1.93; P, 4.85%. The third band afforded $[Os_4(CO)_{10}(\mu_3\text{-}Se)_4(\mu\text{-dppm})]$ (**5**) (0.008 g, 5%) as yellow crystals from hexane/CH_2Cl_2 at −4 °C. IR (νCO, CH_2Cl_2): 2091 m, 2075 s, 2017 s, 1992 vs, 1948 m cm^{-1}; ^{1}H-NMR (CD_2Cl_2): δ 7.36 (m, 20H), 4.07 (t, 2H, $J = 11.6$ Hz) ppm; $^{31}P\{^1H\}$-NMR (CD_2Cl_2): δ −7.4(s) ppm; mass spectrum: m/z 1740. Anal. Calc. for $C_{35}H_{22}O_{10}Os_4P_2Se_4$: C, 24.14; H, 1.28; P, 3.56. Found: C, 24.32; H, 1.45; P, 3.72%.

2.2. Reaction of $[Os_3(CO)_{10}(MeCN)_2]$ with dppmSe

To a dichloromethane solution (30 ml) of $[Os_3(CO)_{10}(MeCN)_2]$ (0.225 g, 0.241 mmol) was added dppmSe (0.168 g, 0.363 mmol) and the reaction mixture was stirred at room temperature for 48 h. The solvent was removed under reduced pressure and the residue was chromatographed by TLC on silica gel. Elution with hexane/acetone (3:2, v/v) developed three major and several very minor bands. The faster moving yellow band gave $[Os_2(CO)_6(\mu\text{-Se})(\mu\text{-dppm})]$ (**6**) (0.032 g, 13%) as yellow crystals after recrystallization from hexane/CH_2Cl_2 at room temperature. IR (νCO, CH_2Cl_2): 2098 w, 2073 vs, 2035 vs, 1998 m, 1977 w, 1963 m cm^{-1}; ^{1}H-NMR ($CDCl_3$): δ 7.43 (m, 20H), 4.95 (m, 1H), 3.36 (m, 1H) ppm; methylene signals are "apparent quartets" due to overlapping triplets. $^{31}P\{^1H\}$-NMR ($CDCl_3$): δ −23.6(s) ppm; mass spectrum: m/z 1012. Anal. Calc. for $C_{31}H_{22}O_6Os_2P_2Se$: C, 36.80; H, 2.20; P, 6.12. Found: C, 36.92; H, 2.35; P, 6.12%. The second band gave **3** (0.0075 g, 24%) while the third band yielded **4** (0.013 g, 4%). Each of the minor bands gave a small amount of unidentified product.

2.3. Reaction of $[Os_3(CO)_{10}(MeCN)_2]$ with $dppmSe_2$

A benzene solution (100 ml) of $[Os_3(CO)_{10}(MeCN)_2]$ (0.205 g, 0.220 mmol) and $dppmSe_2$ (0.196 g, 0.361 mmol) was heated to reflux for 2 h. The solvent was removed under reduced pressure and the residue was chromatographed by TLC on silica gel. Elution with hexane/CH_2Cl_2 (7:3, v/v) developed two bands. The first band yielded **3** (0.079 g, 27%), while the second band afforded **5** (0.016 g, 7%) as orange crystals after recrystallization from hexane/CH_2Cl_2 at room temperature.

2.4. Reaction of **3** with Me_3NO

A toluene solution (30 ml) of **3** (0.126 g, 0.096 mmol) and anhydrous Me_3NO (0.011 g, 0.146 mmol) was heated at 80 °C for 20 min during which time the color changed from orange to green. The reaction solution was filtered through a short silica gel column to remove excess anhydrous Me_3NO. The solvent was removed under reduced pressure and the residue was chromatographed by TLC on silica gel. Elution with hexane/CH_2Cl_2 (3:2, v/v) developed a green band which afforded $[Os_6(CO)_{12}(\mu_3\text{-Se})_4(\mu\text{-dppm})_2]$ (**7**) (0.093 g, 75%), as green crystals after recrystallization from heptane/CH_2Cl_2 at room temperature. IR (νCO, CH_2Cl_2) 2031 w, 2015 vs, 1981 s, 1950 s, 1894 w cm^{-1}; ^{1}H-NMR ($CDCl_3$): δ 7.29 (m, 40H), 4.28 (t, 4H) ppm; $^{31}P\{1H\}$-NMR (CD_2Cl_2): δ −10.92 (d, J = 15.6), −11.11 (d, J = 17.2) ppm; mass spectrum: m/z 2562. Anal. Calc. for $C_{62}H_{44}O_{12}Os_6P_4Se_4$: C, 29.06; H, 1.73; P, 4.84. Found: C, 29.35; H, 1.27, P, 4.96%.

2.5. Reaction of **3** with PPh_3 in presence of Me_3NO

To a dichloromethane solution of **3** (0.045 g, 0.034 mmol) and PPh_3 (0.018 g, 0.068 mmol) was added dropwise a solution of anhydrous Me_3NO (0.005 g, 0.067 mmol) in the same solvent (10 ml) over a period of 10 min. The reaction mixture was stirred at room temperature for 3 h during which time analytical TLC indicated complete consumption of **3**. Work-up followed by chromatographic separation as above developed two bands. The yellow band yielded $[Os_3(CO)_6(\mu_3\text{-Se})_2(\mu\text{-dppm})(PPh_3)]$ (**8**) (0.014 g, 26%) as yellow crystals after recrystallization from hexane/CH_2Cl_2 at 4 °C. IR (νCO, CH_2Cl_2) 2014 s, 1989 vs, 1941 vs, 1928 m cm^{-1}; ^{1}H-NMR (CD_2Cl_2): δ 7.31 (m, 20H), 5.36 (q, 1H, J = 11.4 Hz), 3.81 (q, 1H, J = 11.2 Hz) ppm; $^{31}P\{1H\}$-NMR (CD_2Cl_2): δ 13.1(s), −6.8 (d, J = 40.0 Hz), −19.1 (d, J = 40.0 Hz) ppm; mass spectrum: m/z 1542. Anal. Calc. for $C_{49}H_{37}O_6Os_3P_3Se_2$: C, 38.13; H, 2.42; P, 6.02. Found: C, 38.27; H, 2.52; P, 6.15%. The green band afforded **7** (0.009 g, 20%).

2.6. Reaction of **7** with CO

Carbon monoxide gas was bubbled through a refluxing heptane solution (30 ml) of **7** (0.015 g, 0.006 mmol) for 3 h. The color changed from green to yellow. The solvent was removed under reduced pressure and the residue was chromatographed by TLC on silica gel. Elution with hexane/CH_2Cl_2 (3:1, v/v) gave a single band which afforded **3** (0.012 g, 80%).

2.7. Attempted reaction of **1** with elemental selenium

To a toluene solution of **1** (0.0026 g, 0.021 mmol) was added black selenium (0.004 g, 0.051 mmol) and the reaction mixture was heated to reflux for 3 h. Usual work-up followed by chromatographic separation afforded several very minor bands each of which afforded very small amount of intractable material.

2.8. X-ray structural determination of **4** and **6**

Crystallographic and other experimental data are summarized in Table 1. Crystallographic data were collected at 120 K, using a Bruker-Nonius CCD area detector diffractometer and Mo–Kα radiation (λ = 0.71073 Å). Data collection and processing were carried out using the programs COLLECT [23] and DENZO [24]. Empirical absorption corrections were applied to the data sets using multiple and symmetry-related data measurements via the program SORTAV [25,26]. The unit cells were indexed from all observed reflections in a

Table 1
Crystallographic data for **3**, **4**, **6**, **7** and **8**

	3	**4**·CH_2Cl_2	**6**	**7**	**8**
Empirical formula	$C_{32}H_{22}O_7Os_3P_2Se_2$	$C_{33}H_{22}O_8Os_3P_2Se$	$C_{31}H_{22}O_6Os_2P_2Se$	$C_{62}H_{44}C_{10}O_{12}Os_6P_4Se_3$	$C_{48}H_{35}O_6Os_3P_3Se_2$
Formula weight	1308.96	1342.93	1011.79	2482.93	1529.19
Temperature (K)	293(2)	120(2)	150(2)	293(2)	293(2)
Wavelength (Å)	0.71073	0.71073	0.71073	0.71073	0.71073
Crystal system	Triclinic	Triclinic	Monoclinic	Monoclinic	Monoclinic
Space group	$P\bar{1}$	$P\bar{1}$	$C2/c$	$P2_1/c$	$P2_1/n$
Unit cell dimensions					
a (Å)	10.1870(10)	9.07250(10)	22.6088(2)	18.234(8)	14.736(3)
b (Å)	11.1430(10)	10.70790(10)	12.44590(10)	19.37(2)	12.301(4)
c (Å)	17.873(2)	19.0488(3)	24.2228(3)	20.396(10)	26.897(7)
α (°)	74.580(10)	86.4630(10)	90	90.01(7)	90
β (°)	84.660(10)	86.5990(10)	115.7778(6)	75.21(3)	98.61(2)
γ (°)	64.400(10)	81.5570(10)	90	90.03(5)	90
V (Å^3)	1763.2(3)	1824.63(4)	6137.70(11)	6964(9)	4821(2)
Z	2	2	8	4	4
Absorption coefficient (cm^{-1})	12.982	11.701	9.606	12.619	9.544
Crystal size (mm^3)	0.20 × 0.25 × 0.30	0.45 × 0.16 × 0.16	0.25 × 0.08 × 0.06	0.163 × 0.09 × 0.06	0.34 × 0.17 × 0.13
Reflections collected	4014	22402	42205	3604	3174
Independent reflections	3270 [$R_{int} = 0.0240$]	6399 [$R_{int} = 0.1223$]	7013 [$R_{int} = 0.0472$]	2807 [$R_{int} = 0.0822$]	2295 [$R_{int} = 0.0659$]
Refinement method	Full-matrix least-squares on F^2	Full-matrix least-squares on F^2	Full-matrix least-squares on F^2	Full-matrix least-squares on F^2	Full-matrix least-squares on F^2
Goodness-of-fit on F^2	1.089	0.957	1.072	1.065	1.104
Final R indices [$I > 2\sigma(I)$]	$R_1 = 0.0353$, $wR_2 = 0.0909$	$R_1 = 0.0742$, $wR_2 = 0.1634$	$R_1 = 0.0252$, $wR_2 = 0.0550$	$R_1 = 0.0677$, $wR_2 = 0.1601$	$R_1 = 0.0621$, $wR_2 = 0.1575$
R indices (all data)	$R_1 = 0.0382$, $wR_2 = 0.936$	$R_1 = 0.0782$, $wR_2 = 0.1669$	$R_1 = 0.0315$, $wR_2 = 0.0575$	$R_1 = 0.1093$, $wR_2 = 0.1844$	$R_1 = 0.0766$, $wR_2 = 0.1762$

$R_1 = \Sigma||F_o| - |F_c||/\Sigma|F_o|$, $wR_2 = [\Sigma[w(F_o^2 - F_c^2)/\Sigma[w(F_o^2)^2]]^{1/2}$, $w = 1/[\sigma^2(F_o^2) + (a_1P)^2 + a_2P]$ where $P = (F_o^2 + F_c^2)/3$.

θ-range of 10° and refined using the entire data sets. The structures were solved by direct methods (SHELXS-97) [27] and refined on F^2 by full-matrix least-squares (SHELXL-97) [28] using all unique data. All non-hydrogen atoms were refined anisotropically. Hydrogen atoms were included in calculated positions (riding model) with U_{iso} set at 1.2 times the U_{eq} of the parent atom. Selected bond lengths and angles for **4** and **6** are given in Tables 3 and 4, respectively.

2.9. X-ray structural determination of 3, 7 and 8

Crystallographic and other experimental data are summarized in Table 1. Crystallographic data were collected at 296 K, using a Bruker P4 diffractometer with Mo–Kα radiation ($\lambda = 0.71073$ Å). Data collection and processing were carried out using XSCANS [29]. The unit cells were indexed on low angle reflections and refined from 25 reflections in a θ-range of 12°–13°. The structures were solved by direct methods (SHELXS-97) [27] and refined on F^2 by full-matrix least-squares (SHELXL-97) [28], utilized as incorporated in the WINGX [30] program package using all unique data. All non-hydrogen atoms for **3** were refined anisotropically. Carbon atoms for **7** and **8** were refined isotropically, with all other atoms refined anisotropically. Hydrogen atoms were included in calculated positions (riding model) with U_{iso} set at 1.2 times the U_{eq} of the parent atom. Selected bond lengths and angles for **3** and **7** and **8** are given in Tables 2, 5 and 6, respectively.

3. Results and discussion

The 46 electron cluster [(μ-H)$Os_3(CO)_8${Ph_2PCH_2-P(Ph)C_6H_4}] (**2**) reacts with elemental selenium at 80 °C to give, after chromatographic separation, two triosmium clusters and one tetraosmium cluster, [$Os_3(CO)_7(\mu_3$-Se)$_2$(μ-dppm)] (**3**), [$Os_3(CO)_7(\mu_3$-CO)(μ_3-Se)(μ- dppm)] (**4**) and [$Os_4(CO)_{10}(\mu_3$-Se)$_4$(μ-dppm)] (**5**) in 20, 47 and 5% yields, respectively (Scheme 1). Compound **3** has been characterized by a combination of infrared, ^{1}H- and ^{31}P{^{1}H}-NMR spectroscopies, FAB mass spectrometry, elemental analysis and a single-crystal X-ray diffraction study. The molecular structure of **3** is shown in Fig. 1, and selected bond

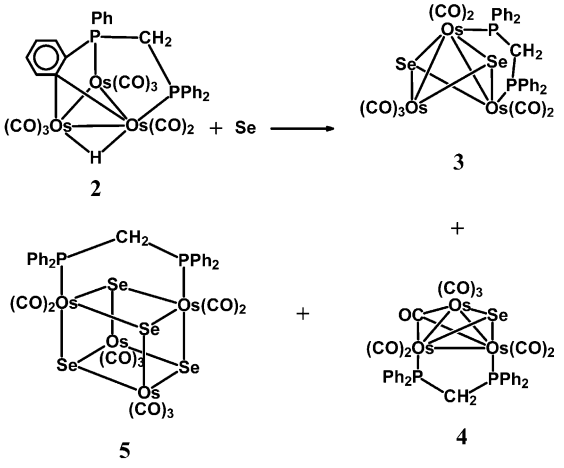

Scheme 1.

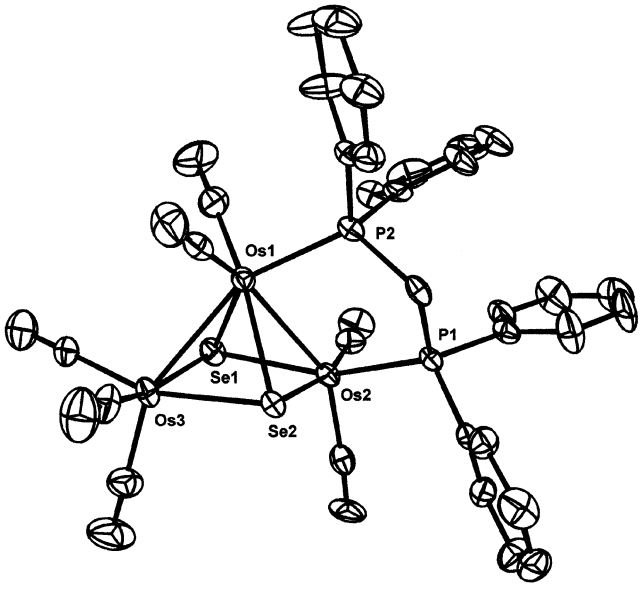

Fig. 1. Molecular structure of $[Os_3(CO)_7(\mu_3\text{-}Se)_2(\mu\text{-}dppm)]$ (**3**).

Table 2
Selected interatomic distances (Å) and angles (°) for **3**

Interatomic distances	
s(1)–Os(2)	2.8742(7)
Os(1)–Os(3)	2.8330(7)
Os(1)–Se(1)	2.5404(13)
Os(1)–Se(2)	2.5757(13)
Os(2)–Se(1)	2.4773(13)
Os(2)–Se(2)	2.5277(12)
Os(3)–Se(1)	2.4987(14)
Os(3)–Se(2)	2.5264(12)
Os(1)–P(2)	2.313(3)
Os2–P(1)	2.356(3)
Os(2)–Os(3)	3.812
Se(1)–Se(2)	3.246
Os–C(CO) (average)	1.89(2)
C–O (average)	1.13(2)
P–C (average)	1.84(2)
Interatomic angles	
Se(1)–Os(1)–Se(2)	74.75(4)
Se(1)–Os(1)–Se(3)	55.10(3)
Se(2)–Os(1)–Se(3)	55.45(3)
P(2)–Os(1)–Os(2)	81.35(7)
Se(1)–Os(1)–Os(2)	54.03(3)
Se(2)–Os(1)–Os(2)	54.93(3)
Os(3)–Os(1)–Os(2)	83.80(2)
P(1)–Os(2)–Se(1)	153.96(8)
P(1)–Os(2)–Se(2)	85.65(8)
Se(1)–Os(2)–Se(2)	80.85(4)
P(1)–Os(2)–Os(1)	97.92(7)
Se(1)–Os(2)–Os(1)	56.09(3)
Se(2)–Os(2)–Os(1)	56.09(3)
Se(1)–Os(3)–Se(2)	80.46(4)
Se(1)–Os(3)–Os(1)	56.49(3)
Se(2)–Os(3)–Os(1)	57.11(3)
Os(3)–Se(2)–Os(2)	97.90(4)
Os(3)–Se(2)–Os(1)	67.45(3)
Os(2)–Se(2)–Os(1)	68.55(3)
Os(2)–Se(1)–Os(1)	69.88(3)
Os(3)–Se(1)–Os(1)	68.41(3)

distances and angles are collected in Table 2. The molecule consists of an open cluster of three metal atoms with two metal–metal bonds and seven linear terminal carbonyl ligands. Two osmium atoms, Os(1) and Os(2), are each bound to two terminal carbonyls and to a phosphorus atom from the dppm ligand; Os(3) is bound to three terminal carbonyls. The osmium–osmium bonding distances in **3** are Os(1)–Os(3) = 2.8330(7) Å and Os(1)–Os2 = 2.8742(7) Å, similar to the average Os–Os distances observed in $[Os_3(CO)_{12}]$ {2.877(3) Å} [31]. The corresponding distances in **1** are 2.7910(11) and 2.8412(12) Å [20]. The non-bonding osmium–osmium distance {Os(2)–Os(3) = 3.812 Å} is significantly longer than that observed in $[Os_3(CO)_9(\mu_3\text{-}S)_2]$ {3.662(1) Å} [32], $[Os_3(CO)_9(\mu_3\text{-}Se)_2]$ {3.718 Å} [33] and $[Os_3(CO)_8(\mu_3\text{-}S)_2(CS)]$ {3.644 Å} [32]. This observation is consistent with the argument that the substitution of carbonyls with more weakly π-acidic phosphine ligands results in an increase in electron density at the metal centers increasing electron–electron repulsion between the non-bonded osmium atoms [34,35]. Alternatively, the expansion of the cluster could be explained on the basis of steric interactions. In this case, the substitution of a bulky ligand for a less bulky one would also result in an increase in the non-bonded Os–Os distance [36]. In this cluster, there are two triply bridging (non-bonded) selenium atoms (the separation between these atoms is 3.246 Å) and one doubly bridging dppm ligand. In contrast, in $[Fe_3(CO)_7(\mu_3\text{-}Se)_2(\mu\text{-}dppm)]$ [7b], $[Fe_3(CO)_7(\mu_3\text{-}Se)_2(\mu\text{-}dppe)]$ [7b], $[Fe_3(CO)_7(\mu_3\text{-}Se)_2(\mu\text{-}dppfc)]$ [7b], $[Ru_3(CO)_7(\mu_3\text{-}Se)_2(\mu\text{-}dppm)]$ [7c], $[Ru_3(CO)_7(\mu_3\text{-}Se)_2(\mu\text{-}dppa)]$ [3a] and $[Ru_3(CO)_7(\mu3\text{-}Se)_2(\mu\text{-}dppe)]$ [7d] the bidentate phosphine ligand bridges the two basal metal atoms in the axial positions; the dppm ligand in **3** bridges one of the bonded pair of osmium atoms, Os(1) and Os(3). The Os(2)–P(1) distance {2.356(3) Å, equatorial, transoid to Se} is

significantly longer than the Os(1)–P(2) distance {2.313(3) Å, axial, transoid to Os}. This observation is consistent with that suggested by Tiripicchio et al. in which the M–P interaction in the 50-electron M_3S_2 *nido*-clusters experiences a *trans* stabilizing effect [7d]. The structure can be envisaged as a square-pyramidal Os_3Se_2 core with two Os atoms and the Se atoms alternating in the basal positions and third osmium atom at the apex of the pyramid. The Os–Se distances to the central seven coordinated metal atom Os(1), {Os(1)–Se(1) = 2.5404(13) Å and Os(1)–Se(2) = 2.5707(13) Å} are significantly longer than those to the external six-coordinate metal atoms Os(2) and Os(3) {Os(2)–Se(1) = 2.4773(13), Os(2)–Se(2) = 2.5277(12), Os(3)–(1) = 2.4987(14), Os(3)–Se(2) = 2.5264(12) Å}. A similar structural feature has also been observed for the unsubstituted selenium and sulfur analogs $[Os_3(CO)_9(\mu_3\text{-}S)_2]$ [32] and $[Os_3(CO)_9(\mu_3\text{-}Se)_2]$ [33].

The spectroscopic data of **3** are consistent with the solid-state structure. The mass spectrum of **3** confirms the formula $[Os_3(CO)_7(\mu_3\text{-}Se)_2(\mu\text{-}dppm)]$, exhibiting the molecular ion peak at *m*/*z* 1308 and peaks due to the sequential loss of seven carbonyl groups. The infrared spectrum of **3** exhibits peaks at 2067 vs, 2000 vs, 1985 sh, 1944 s and 1869 w cm^{-1}, indicating the presence of only terminally bonded carbonyls. The $^{31}P\{^1H\}$-NMR spectrum of **3** in $CDCl_3$ shows two doublets at δ −7.6 (d, J = 92.4 Hz) and −23.1 (d, J = 92.4 Hz) ppm. This implies the presence of only one isomer with the phosphorus nuclei in inequivalent environments. The ^{1}H-NMR spectrum shows two multiplets at δ 3.93 and 5.93 ppm for the methylene protons and a series of well-separated multiplets centered at δ 6.74, 7.05, 7.13, 7.41 and 7.80 ppm with a relative intensity ratio of 2:2:1:13:2, respectively, for the phenyl protons of the dppm ligand.

The cluster **4** has been characterized from IR, ^{1}H-, $^{31}P\{^1H\}$-NMR and mass spectroscopic data as well as by single-crystal X-ray diffraction studies. The infrared spectrum in the carbonyl stretching region consists of bands typical of terminal carbonyls, and one strong band at 1734 cm^{-1} consistent with the triply bridging carbonyl ligand. The molecular structure of **4** is shown in Fig. 2 and selected bond distances and angles are listed in Table 3. Compound **4** consists of a triangular cluster of three mutually bonded osmium atoms with seven terminal carbonyls and a triply bridging carbonyl ligand, a triply bridging selenido ligand and a bridging dppm ligand. The geometry of the Os_3Se core in which an isosceles triangle of osmium atoms is symmetrically capped by the Se atom {Os(2)–Se(1) = 2.5221(13) Å, Os(1)–Se(1) = 2.5123(14) Å and Os(3)–Se(1) = 2.5302(15) Å} can be described as tetrahedral. In contrast, the triply bridging carbonyl ligand is bonded asymmetrically to the Os_3 triangle {Os(1)–C(1) = 2.221(15) Å, Os(3)–C(1) = 2.160(14) Å and Os(2)–C(1) = 2.190(13) Å}. The Os(1)–Os(2) and Os(1)–

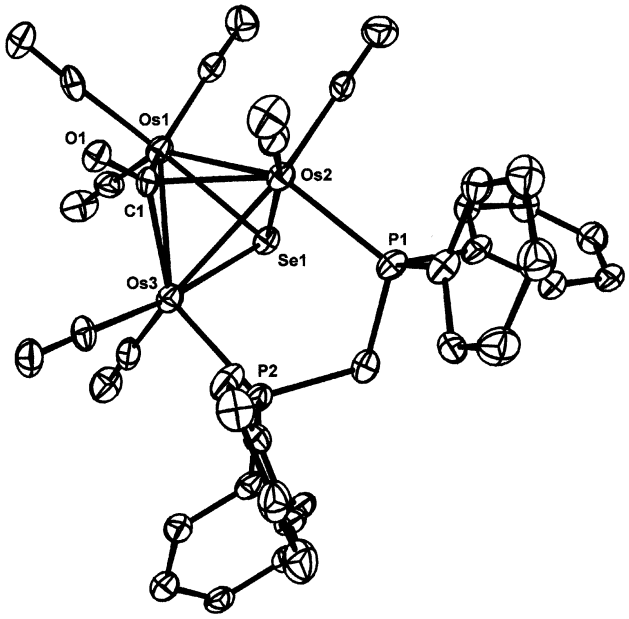

Fig. 2. Molecular structure of $[Os_3(CO)_7(\mu_3\text{-}CO)(\mu_3\text{-}Se)(\mu\text{-}dppm)]$ (**4**).

Os(3) edges are of comparable length {2.8442(7) and 2.8556(8) Å, respectively} whereas Os(2)–Os(3) {2.8274(8) Å} is slightly shorter. All three Os–Os distances are shorter than that in the parent carbonyl complex $[Os_3(CO)_{12}]$ {2.877(3) Å} [31]. The triply bridging selenido and the carbonyl ligands lie on opposite sides of the Os_3 triangle resulting in a trigonal bipyramidal geometry for the $Os_3(Se)(CO)$ core. The dppm ligand bridges the shortest Os(2)–Os(3) edge of the triangle. Of the seven terminal carbonyl ligands two bonded to each of Os(2) and Os(3) and three to Os(1). The Os–P bond distances in **4** {Os(2)–P(1) = 2.342(3) Å and Os(3)–P(2) = 2.326(3) Å} are comparable with the corresponding distances in **1** {2.332(3) and 2.312(3) Å} [37]. The compound contains 48 valence electrons, consistent with three metal–metal bonds. Overall, the structure of **4** is similar to that of the sulfur analog $[Os_3(CO)_7(\mu_3\text{-}CO)(\mu_3\text{-}S)(\mu\text{-}dppm)]$, synthesized from the reaction of **1** with thiourea [20].

The tetranuclear cluster **5** is probably formed either by the self-assembly of two dinuclear Os_2Se_2 groups, derived from **3** by loss of a mononuclear metal fragment or by addition of an $Os(CO)_n$ fragment to **3** along with addition of two further Se atoms. The latter scenario is consistent with the observation that there is only a single diphosphine ligand in the complex. The structural assignment for **5** is based primarily on infrared spectroscopic data. The infrared spectrum of **5** exhibits bands at 2091 s, 2075 s, 2017 vs, 1992 w and 1948 w cm^{-1}, which are characteristic of terminal carbonyl ligands. No bands are observed in the 1700–1900 cm^{-1} region, indicating that no bridging carbonyls are present in the complex. This structural assignment is supported by comparison with ν(CO) the frequencies observed for the

Table 3
Selected interatomic distances (Å) and angles (°) for **4**

Interatomic distances	
Os(1)–Os(2)	2.8442(7)
Os(2)–Os(3)	2.8274(8)
Os(1)–Os(3)	2.8556(8)
Os(2)–Se(1)	2.5221(13)
Os(1)–Se(1)	2.5123(14)
Os(3)–Se(1)	2.5302(15)
Os(1)–C(1)	2.221(15)
Os(3)–C(1)	2.160(14)
Os(2)–C(1)	2.190(13)
Os(2)–P(1)	2.342(3)
Os(3)–P(2)	2.326(3)
Os–C(terminal) (average)	1.91(2)
C–O (average)	1.14(2)
P–C (average)	1.82(2)
Interatomic angles	
Os(1)–Se(1)–Os(3)	69.07(3)
Os(1)–Se(1)–Os(2)	68.88(3)
Os(2)–Se(1)–Os(3)	68.16(3)
O(1)–C(1)–Os(2)	133.0(9)
O(1)–C(1)–Os(1)	129.2(9)
O(1)–C(1)–Os(1)	80.5(4)
O(1)–C(1)–Os(3)	131.9(9)
Os(3)–C(1)–Os(2)	81.3(4)
Os(3)–C(1)–Os(1)	81.4(4)
C(2)–Os(1)–Se(1)	94.6(4)
C(3)–Os(1)–Se(1)	94.8(4)
C(7)–Os(2)–Se(1)	166.4(4)
P(1)–Os(2)–Se(1)	87.80(8)
C(5)–Os(3)–Se(1)	172.4(4)
C(1)–Os(3)–Se(1)	91.1(3)
C(4)–Os(1)–Se(1)	170.7(4)
C(1)–Os(1)–Se(1)	90.2(3)
C(8)–Os(2)–Se(1)	101.3(4)
C(1)–Os(2)–Se(1)	90.9(3)
C(6)–Os(3)–Se(1)	91.3(4)
P(2)–Os(3)–Se(1)	94.01(8)
Os(2)–Os(1)–Os(3)	59.490(16)
Os(3)–Os(2)–Os(1)	60.460(16)
Os(2)–Os(3)–Os(1)	60.050(16)
Se(1)–Os(1)–Os(2)	55.72(3)
Se(1)–Os(1)–Os(1)	55.40(3)
Se(1)–Os(3)–Os(2)	55.78(3)
Se(1)–Os(1)–Os(3)	55.76(3)
Se(1)–Os(2)–Os(3)	56.06(3)
Se(1)–Os(3)–Os(2)	55.17(3)
P(1)–Os(2)–Os(3)	95.57(8)
P(2)–Os(3)–Os(2)	89.77(8)

ruthenium analog, $[Ru_4(CO)_{10}(\mu_3\text{-}Se)_4(\mu\text{-}dppm)]$ which was synthesized by Predieri et al., from the reaction of $[Ru_3(CO)_{12}]$ with dppmSe in the presence of Me_3NO at 110 °C and unambiguously characterized by single-crystal X-ray diffraction studies [7a]. The FAB mass spectrum of **5** exhibits the molecular ion peak at *m*/*z* 1740 followed by sequential loss of 10 carbonyl ligands. This typical fragmentation pattern suggests that **5** is a decacarbonyl tetraosmium complex. The $^{31}P\{^1H\}$-NMR spectrum contains a singlet at δ −7.4 ppm indicating equivalent ^{31}P nuclei. Consistent with this, the ^1H-NMR spectrum of **5** in the aliphatic region contains a triplet at δ 4.07 ppm indicating that the two phosphorus atoms and the two methylene hydrogen atoms of the bridging dppm ligand are equivalent. All of the spectroscopic data for **5** are very similar to those of the corresponding ruthenium analog $[Ru_4(CO)_{10}(\mu_3\text{-}Se)_4(\mu\text{-}dppm)_2]$ [7a], indicating that they are isostructural. Compound **5** could not be characterized structurally by X-ray diffraction due to the lack of X-ray quality crystals.

Treatment of $[Os_3(CO)_{10}(MeCN)_2]$ with dppmSe at room temperature leads to the formation of the dinuclear compound $[Os_2(CO)_6(\mu\text{-}Se)(\mu\text{-}dppm)]$ [8] and the trinuclear compounds **3** and **4** (Scheme 2) in 13, 24 and 4% yields, respectively. Minor uncharacterized products were also obtained. The dinuclear compound is probably produced by decomposition of the Os_3Se core in **4** through an inner reduction–oxidation process.

Compound **6** was initially characterized by elemental analysis, IR, ^1H-NMR, $^{31}P\{^1H\}$-NMR and mass spectroscopic data. The infrared spectrum of **6** exhibits bands at 2073 vs, 2035 vs, 1998 m, 1977 w and 1963 m cm^{-1}, indicating that all the CO groups are terminally bonded. The mass spectrum contains a parent ion at *m*/*z* 1012 and in addition stepwise loss of six carbonyl groups has been observed. The ^1H-NMR spectrum contains two multiplets centered at δ 4.95 and 3.36 ppm due to the methylene protons and a multiplet centered at δ 7.43 ppm for phenyl protons of the dppm ligand. The $^{31}P\{^1H\}$-NMR shows a singlet at δ −19.7 ppm, indicating that the ^{31}P nuclei are equivalent. In spite of this apparent equivalency, the number of carbonyl stretching frequencies observed in CH_2Cl_2 presents the possibility of isomers in solution in which the dppm ligand adopts "up" and "down" conformations. It is likely that the isomers interconvert more rapidly than can be detected on the NMR time scale. The structure of **6** has been confirmed by single-crystal X-ray diffraction studies; its molecular structure is shown in Fig. 3 and selected bond distances and bond angles are presented in Table 4. The compound consists of two osmium atoms with six linear terminal carbonyl ligands, three bonded to each osmium atom, one doubly bridging selenido ligand and a bridging dppm ligand. The Os(1)–Os(2) bond length is 2.8933(2) Å, which is slightly longer than that found in $[Os_3(CO)_{12}]$ {2.877(3) Å} [31]. The Os(1)–Se(1) and Os(2)–Se(1) bond distances of 2.5471(4) and 2.518(4) Å are comparable to the Os–Se bond distances in **3**, **4** and other triosmium

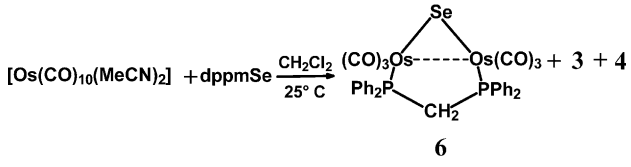

Scheme 2.

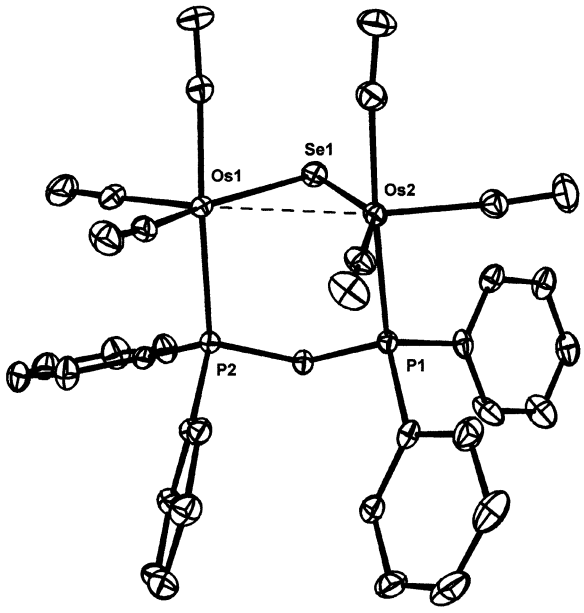

Fig. 3. Molecular structure of $[Os_2(CO)_6(\mu\text{-Se})(\mu\text{-dppm})]$ (**6**).

Table 4
Selected interatomic distances (Å) and angles (°) for **6**

Interatomic distances	
Os(1)–Os(2)	2.8933(2)
Os(1)–Se(1)	2.5471(4)
Os(2)–Se(1)	2.5418(4)
Os(2)–P(1)	2.4041(9)
Os(1)–P(2)	1.4004(9)
Os(1)–C(1)	1.906(4)
Os(1)–C(3)	1.932(4)
Os(2)–C(6)	1.899(4)
Os(2)–C(5)	1.908(4)
Os(2)–C(4)	1.933(4)
Os(1)–C(2)	1.917(5)
C–O (average)	1.13(2)
P–C (average)	1.83(1)
Interatomic angles	
Se(1)–Os(1)–Os(2)	55.265(9)
P(1)–Os(2)–Os(1)	69.297(10)
Se(2)–Os(2)–Os(1)	55.438(9)
Os(2)–Se(1)–Os(1)	69.297(10)
P(2)–Os(1)–Se(1)	90.51(2)
P(2)–Os(1)–Os(2)	88.90(2)
Se(1)–Os(2)–Os(1)	55.438(9)

compounds containing bridging selenido ligands 38. The dppm ligand bridges two osmium atoms in the axial position and the Os–P bond distances {Os(1)–P(2) = 2.4004(9) Å and Os(2)–P(1) = 2.4041(9) Å} are significantly longer than those found in $[Os_3(CO)_7(\mu_3\text{-S})_2(\mu\text{-dppm})]$ (**3**), {Os(1)–P(1) = 2.286(3) Å and Os(2)–P(2) = 2.302(3) Å}. The doubly bridging selenido ligand donates two electrons and the bridging dppm ligand donates four electrons to make **6** a 34 electron valence-saturated bimetallic compound. In contrast, the reaction of $[Os_3(CO)_{10}(MeCN)_2]$ with $dppmSe_2$ at 80 °C is quite selective giving **3** and **5** in 27 and 7% yields, respectively.

The triply bridging chalcogenido ligands with lone pairs of electrons have been considered to be ideal species for cluster growth reactions. These ligands facilitate the formation of higher nuclearity clusters by using the lone pair of electrons to form coordinative interactions to electron-deficient metal groupings. Of the chalcogen elements, the triply bridging sulfido ligand has been extensively used for the purpose of cluster growth reactions [2]. The much larger tellurido ligand has also been shown to stabilize triangular and square arrays of metal atoms [3b,39]. In comparison, few studies have been performed using the capping selenido ligand for cluster growth reactions [7c]. By analogy with the formation of $[Os_6(CO)_{16}(\mu_3\text{-S})_4]$ [30] by photolysis of $[Os_3(CO)_9(\mu_3\text{-S})_2]$ and $[Ru_6(CO)_{12}(\mu_3\text{-Se})_4(\mu\text{-dppm})_2]$ [7c] by the reaction of $[Ru_3(CO)_7(\mu\text{-Se})_2(\mu\text{-dppm})]$ with Me_3NO at 110 °C, it was considered that the reaction of **3** with Me_3NO might give the corresponding hexanuclear compound $[Os_6(CO)_{12}(\mu_3\text{-Se})_4(\mu\text{-dppm})_2]$. As expected, treatment of **3** with Me_3NO in toluene at 80 °C affords the novel cluster $[Os_3(CO)_6(\mu_3\text{-Se})_2(\mu\text{-dppm})]_2$ [9] (Scheme 3) as green crystals in 50% yield. Compound **7** has been characterized both spectroscopically and by single-crystal X-ray diffraction studies. The solid-state structure of **7** is shown in Fig. 4 and selected bond distances and angles are collected in Table 5. The compound is believed to be formed by condensation of two $[Os_3(CO)_6(\mu_3\text{-Se})_2(\mu\text{-dppm})]$ units formed by the loss of a carbonyl ligand from **3**. An intriguing structural feature of **7** is that, in contrast to **3** in which the dppm ligand bridges one of the bonding Os–Os edges, both the dppm ligands span the open osmium–osmium edges with two phosphorus atoms occupying equatorial sites on two metal atoms. The molecule may be viewed as an extended array of six osmium atoms with four triply bridging selenido ligands, two bridging dppm ligands and twelve terminal carbonyl ligands, two terminally coordinated to each osmium atom. The internuclear separations in the core of the cluster span a range and suggest the existence of seven metal–metal bonds. The new metal–metal bonds join the two triosmium diselenido fragments. The central portion of the molecule adopts the form of a butterfly tetrahedron

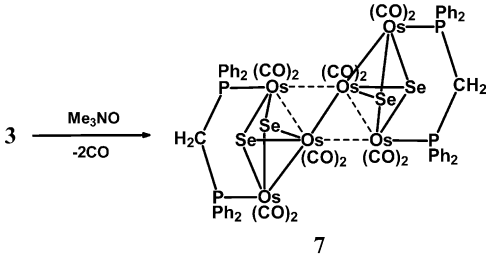

Scheme 3.

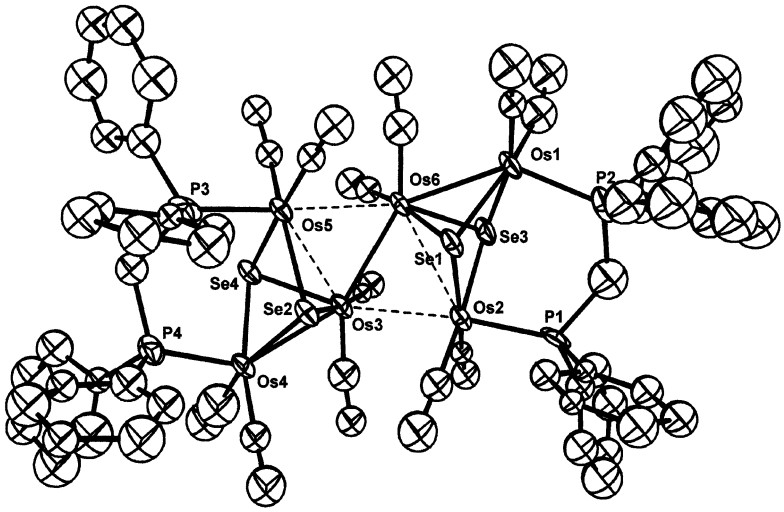

Fig. 4. Molecular structure of $[Os_6(CO)_{12}(\mu_3\text{-}Se)_4(\mu\text{-}dppm)_2]$ (**7**).

of four metal atoms, illustrated by Os(2), Os(3), Os(5) and Os(6). The dihedral angle between the planes defined by Os(3), Os(5), Os(6) and Os(3), Os(6) and Os(2) is 140.5°. This value is comparable to the corresponding dihedral angles in $[Os_6(CO)_{16}(\mu_3\text{-}S)_4]$, {136.3°} [40] and $[Ru_6(CO)_{12}(\mu_3\text{-}Se)_4(\mu\text{-}dppm)_2]$, {141.1°} [7c]. The two remaining metal atoms are linked to the central cluster at the "hinge" atoms one to each, via a metal–metal bond and the bridging selenido ligands. The shortest metal–metal bonds are those involving the external metal atoms, Os(3)–Os(4) = 2.841(4) Å and Os(1)–Os(6) = 2.851(4) Å. and the hinge bond, Os(3)–Os(6) = 2.848(4) Å. The metal–metal bonds around the periphery of the central cluster {Os(2)–Os(6) = 3.042(5), Os(2)–Os(3) = 2.982(4), Os(3)–Os(5) = 3.022(5), Os(5)–Os(6) = 2.988(4) Å}, are significantly longer. The latter distances are comparable to the corresponding osmium–osmium distances in $[Os_6(CO)_{16}(\mu_3\text{-}S)_4]$ [40], ranging from 2.941(1) to 2.973(1) Å, whereas the former are longer than the external metal–metal bond distances in $[Os_6(CO)_{16}(\mu_3\text{-}S)_4]$, which range from 2.789(1) to 2.792(1) Å. The triply bridging selenido ligands are arranged in pairs along diametrically opposed edges of the central cluster and extend to each of the external metal atoms. The Os–Se distances in **7** {2.472(8)–2.551(8) Å} are similar to the Os–Se distances in **3** {2.4773(13)–2.5757(3) Å}. The short bite of the dppm ligands, with an average P–P distance of 3.1973 Å and an average P–C–P angle of 118°, results in the reduction of the non-bonding Os–Os separation from 3.812 Å in **3** to 3.724 and 3.735 Å in **7**. In parallel, the Se–Se distances increase from 3.246 Å in **3** to 3.323 and 3.319 Å in **7**. The Os–P bond distances are comparable to the corresponding distances in **3**. As has been suggested for $[Os_6(CO)_{16}(\mu_3\text{-}S)_4]$ [40] and $[Ru_6(CO)_{12}(\mu_3\text{-}Se)_4(\mu\text{-}dppm)_2]$ [7c], cluster **7**, with seven Os–Os interactions, contains two electrons in excess of the number which formally satisfy the 18 electron rule. These extra electrons occupy low lying anti-bonding orbitals of the central Os_4 core, which correlates well with the lengthening of the four Os–Os bonds around periphery of the central cluster.

Spectroscopic data for **7** are consistent with the solid-state structure. The infrared spectrum of **7** exhibits bands at 2031 w, 2015 vs, 1981 s, 1950 s and 1894 w cm^{-1}, indicating that all of the CO groups are terminal. The ^{1}H-NMR spectrum of **7** in CD_2Cl_2 shows a triplet at δ 4.29 ppm due to equivalent methylene protons, and a multiplet centered at δ 7.29 ppm due to the phenyl protons of the dppm ligand. The $^{31}P\{^1H\}$ spectrum contains two doublets at singlet at δ −10.9 and −11.1 ppm, indicating that the ^{31}P nuclei are not equivalent. The methylene protons appear equivalent at 298 K, but resolve into two resonances at δ 4.56 and 3.88 ppm at 183 K, indicating that the methylene group is fluxional at ambient temperature. The FAB mass spectrum of **7** exhibits the molecular ion peak at m/z 2562 [M^+].

Compound **7** is unusually reactive as exemplified by its reaction with 1 atm of carbon monoxide at 98 °C to regenerate **3** by the cleavage of three unsupported metal–metal bonds.

Treatment of **3** with PPh_3 in presence of Me_3NO as reaction initiator at ambient temperature afforded the substitution product $[Os_3(CO)_6(\mu_3\text{-}Se)_2(\mu\text{-}dppm)(PPh_3)]$ (**8**) (Scheme 4) in 26% yield along with the dimer **7** in 20% yield.

Compound **8** has been characterized by elemental analysis, infrared spectroscopy, ^{1}H-NMR and $^{31}P\{^1H\}$-NMR, as well as by a single-crystal X-ray diffraction study. The infrared spectrum of **8** shows, by comparison with that of **3**, an expected shift of the ν(CO) bands to lower frequencies consistent with greater back-donation into the π* frontier orbitals on CO, due to the increased electron density on the metal atoms from the PPh_3

Table 5
Selected interatomic distances (Å) and angles (°) for **7**

Interatomic distances	
Se(1)–Os(1)	2.532(7)
Se(1)–Os(6)	2.539(8)
Se(1)–Os(2)	2.548(8)
Se(2)–Os(5)	2.534(8)
Se(2)–Os(4)	2.531(7)
Se(2)–Os(3)	2.551(8)
Se(3)–Os(6)	2.483(8)
Se(3)–Os(1)	2.516(8)
Se(3)–Os(2)	2.524(7)
Se(4)–Os(3)	2.472(8)
Se(4)–Os(4)	2.509(8)
Se(4)–Os(5)	2.524(7)
P(1)–Os(2)	2.31(2)
P(2)–Os(1)	2.31(2)
P(3)–Os(5)	2.32(2)
P(4)–Os(4)	2.31(2)
Os(1)–Os(6)	2.851(4)
Os(2)–Os(3)	2.982(4)
Os(2)–Os(6)	3.042(5)
Os(3)–Os(4)	2.841(4)
Os(3)–Os(6)	2.848(4)
Os(3)–Os(5)	3.022(5)
Os(5)–Os(6)	2.998(4)
Se(2)–Se(4)	3.323
Se(1)–Se(3)	3.319
Os(5)–Os(4)	3.724
Os(2)–Os(1)	3.735
Interatomic angles	
Os(1)–Se(1)–Os(6)	68.40(19)
Os(1)–Se(1)–Os(2)	94.7(2)
Os(6)–Se(1)–Os(2)	73.5(2)
Os(5)–Se(2)–Os(4)	94.6(2)
Os(5)–Se(2)–Os(3)	72.9(2)
Os(4)–Se(2)–Os(3)	68.0(2)
Os(6)–Se(3)–Os(2)	74.8(2)
Os(6)–Se(3)–Os(1)	69.5(2)
Os(1)–Se(3)–Os(2)	95.7(3)
Os(3)–Se(4)–Os(4)	69.5(2)
Os(3)–Se(4)–Os(5)	74.4(2)
P(2)–Os(1)–Se(1)	97.5(5)
Se(3)–Os(1)–Se(1)	82.2(2)
P(2)–Os(1)–Os(6)	139.1(5)
Se(3)–Os(1)–Os(6)	54.69(18)
Se(1)–Os(1)–Os(6)	55.92(18)
P(1)–Os(2)–Se(3)	91.8(5)
P(1)–Os(2)–Se(1)	91.5(5)
Se(3)–Os(2)–Se(1)	81.8(2)
P(1)–Os(2)–Os(3)	172.6(5)
Se(3)–Os(2)–Os(3)	95.5(2)
Se(1)–Os(2)–Os(3)	88.55(19)
Os(4)–Se(4)–Os(5)	95.4(3)
P(2)–Os(1)–Se(3)	94.9(6)
Se(1)–Os(2)–Os(6)	53.15(19)
Os(3)–Os(2)–Os(6)	56.41(10)
Se(4)–Os(3)–Se(2)	82.8(3)
Se(4)–Os(3)–Os(4)	55.84(18)
Se(2)–Os(3)–Os(4)	55.67(16)
Se(4)–Os(3)–Os(6)	102.6(2)
Se(2)–Os(3)–Os(6)	89.76(18)
Os(4)–Os(3)–Os(6)	138.73(15)
Se(4)–Os(3)–Os(2)	164.6(2)
Se(2)–Os(3)–Os(2)	91.89(19)

Table 5 (*Continued*)

Os(4)–Os(3)–Os(2)	131.48(14)
Os(6)–Os(3)–Os(2)	62.85(11)
Se(4)–Os(3)–Os(5)	53.56(18)
Se(2)–Os(3)–Os(5)	53.28(18)
Os(4)–Os(3)–Os(5)	78.79(12)
Os(6)–Os(3)–Os(5)	61.34(10)
Os(2)–Os(3)–Os(5)	112.00(13)
P(4)–Os(4)–Se(4)	95.6(5)
P(4)–Os(4)–Se(2)	97.2(5)
Se(4)–Os(4)–Se(2)	82.5(2)
P(4)–Os(4)–Os(3)	139.5(5)
Se(4)–Os(4)–Os(3)	54.61(18)
Se(2)–Os(4)–Os(3)	56.36(18)
P(3)–Os(5)–Se(4)	91.6(5)
P(3)–C(32)–P(4)	119.0(4)
P(1)–C(1)–P(2)	117.0(4)
P(1)–Os(2)–Os(6)	128.7(4)
Se(3)–Os(2)–Os(6)	51.97(19)
P(3)–Os(5)–Se(2)	91.2(5)
Se(4)–Os(5)–Se(2)	82.1(2)
P(3)–Os(5)–Os(6)	170.5(5)
Se(4)–Os(5)–Os(6)	97.3(2)
Se(2)–Os(5)–Os(6)	86.80(19)
P(3)–Os(5)–Os(3)	128.7(5)
Se(4)–Os(5)–Os(3)	51.99(19)
Se(2)–Os(5)–Os(3)	53.80(19)
Os(6)–Os(5)–Os(3)	56.47(10)
Se(3)–Os(6)–Se(1)	82.7(2)
Se(3)–Os(6)–Os(3)	99.9(2)
Se(1)–Os(6)–Os(3)	91.74(18)
Se(3)–Os(6)–Os(1)	55.77(19)
Se(1)–Os(6)–Os(1)	55.68(16)
Os(3)–Os(6)–Os(1)	138.75(15)
Se(3)–Os(6)–Os(5)	161.8(2)
Se(1)–Os(6)–Os(5)	94.32(19)
Os(3)–Os(6)–Os(5)	62.20(11)
Os(1)–Os(6)–Os(5)	135.73(14)
Se(3)–Os(6)–Os(2)	53.20(19)
Se(1)–Os(6)–Os(2)	53.40(19)
Os(3)–Os(6)–Os(2)	60.73(10)
Os(1)–Os(6)–Os(2)	78.60(12)
Os(5)–Os(6)–Os(2)	111.01(12)

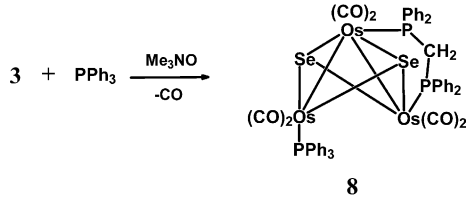

Scheme 4.

ligand, a better σ-donor than CO. The ^{1}H-NMR spectrum of **8** contains two pseudo-quartets centered at δ 5.36 and 3.81 ppm and a multiplet centered at δ 7.31 ppm with a relative intensity ratio of 1:1:35. The ^{31}P{^{1}H}-NMR spectrum contains three resonances of equal intensity, two doublets at δ −6.8 and −19.1 (J = 40.0 Hz) ppm and a singlet at δ 13.1 ppm. The doublets are due to the non-equivalent ^{31}P nuclei of the dppm ligand, while the singlet is due to the PPh_3 ligand. These

NMR data provide strong evidence for the formulation of **8** as $[Os_3(CO)_6(\mu_3\text{-}Se)_2(\mu\text{-}dppm)(PPh_3)]$. This formulation of **8** is also clear from its FAB mass spectrum, which exhibits the molecular ion peak at m/z 1542 as well ions for formulas corresponding to the sequential loss of six carbonyl ligands.

The solid-state structure of **8** is shown in Fig. 5 and selected bond distances and angles are collected in Table 6. The structure consists of an Os_3 triangle involving two metal–metal bonds {Os(1)–Os(3) = 2.864(2) Å and Os(2)–Os(3) = 2.842(2) Å} and a non-bonding metal–metal separation {Os(1)–Os(2) = 3.835 Å}. There are six linear terminal carbonyl ligands, two bonded to each osmium atom, two triply bridging selenido ligands, a bridging dppm ligand and a PPh_3 ligand. The Os(1)–Os(3) edge containing the bridging dppm ligand is slightly longer than the edge which is not bridged. The Os–P bond distances of the dppm ligand in **8** {Os(3)–P(1) = 2.320(9) Å and Os(1)–P(2) = 2.351(10) Å} are close to those observed in **3**. The PPh_3 ligand is coordinated to the unbridged osmium atom Os(2) and the Os(2)–P(3) distance at 2.318(8) Å is comparable to that observed in the related open cluster $[Os_3(CO)_8(\mu_3\text{-}Se)_2(PMe_2Ph)]$ {2.298(3) Å} [4b]. The osmium–selenium distances to the triply bridging selenido ligands {Os(1)/Os(2)/Os(3)–Se(1) = 2.474(5)/2.501(3)/2.526(3) Å and Os(1)/Os(2)/Os(3)–Se(2) = 2.545(3)/2.529(5)/2.564(4) Å} are very similar to those in **3**. The overall structure of **8** is essentially the same as that of **3**, differing only by the substitution of one of the equatorially positioned carbonyl ligands by a triphenylphosphine ligand.

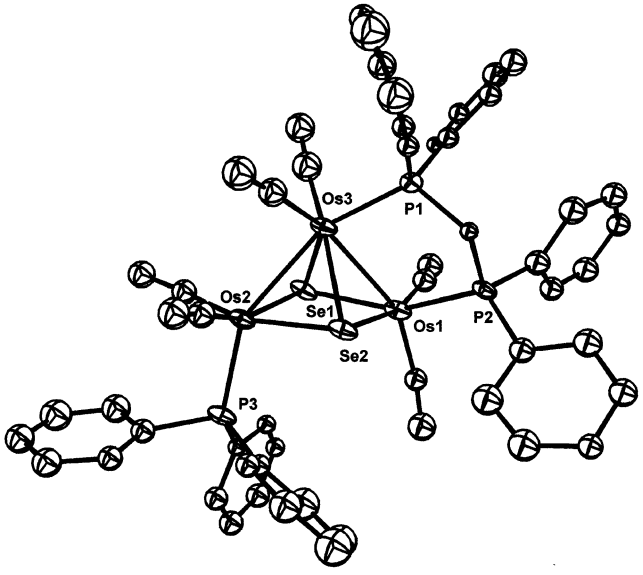

Fig. 5. Molecular structure of $[Os_3(CO)_6(\mu_3\text{-}Se)_2(\mu\text{-}dppm)(PPh_3)]$ (**8**).

Table 6
Selected interatomic distances (Å) and angles (°) for **8**

Interatomic distances	
Se(1)–Os(1)	2.474(5)
Se(1)–Os(2)	2.501(3)
Se(1)–Os(3)	2.526(3)
Se(2)–Os(2)	2.529(5)
Se(2)–Os(1)	2.545(3)
Se(2)–Os(3)	2.564(4)
P(1)–Os(3)	2.320(9)
P(2)–Os(1)	2.351(10)
P(3)–Os(2)	2.318(8)
Os(1)–Os(3)	2.864(2)
Os(2)–Os(3)	2.842(2)
Os(1)–Os(2)	3.835
Se(1)–Se(2)	3.232
P–C (average)	1.81(4)
Os–C(CO) (average)	1.84(4)
C–O (average)	1.19(3)
Interatomic angles	
Os(1)–Se(1)–Os(2)	100.84(15)
Os(1)–Se(1)–Os(3)	69.91(11)
Os(2)–Se(1)–Os(3)	68.85(9)
Os(2)–Se(2)–Os(1)	98.18(13)
Os(2)–Se(2)–Os(3)	67.83(11)
Os(1)–Se(2)–Os(3)	68.19(9)
P(2)–Os(1)–Se(1)	153.8(2)
P(2)–Os(1)–Se(2)	90.7(2)
Se(1)–Os(1)–Se(2)	80.19(13)
P(2)–Os(2)–Os(3)	98.7(2)
Se(1)–Os(1)–Os(3)	55.88(8)
Se(2)–Os(1)–Os(3)	56.22(9)
P(3)–Os(2)–Se(1)	107.8(2)
P(3)–Os(2)–Se(2)	98.4(3)
Se(1)–Os(2)–Se(2)	79.99(13)
P(3)–Os(2)–Os(3)	150.2(3)
Se(1)–Os(2)–Os(3)	55.97(8)
Se(2)–Os(2)–Os(3)	56.69(9)
P(1)–Os(3)–Se(2)	95.4(3)
Se(1)–Os(3)–Se(2)	78.87(12)
P(1)–Os(3)–Os(2)	149.9(2)
Se(1)–Os(3)–Os(2)	55.18(8)
Se(2)–Os(3)–Os(2)	55.49(11)
P(1)–Os(3)–Os(1)	84.1(2)
Se(1)–Os(3)–Os(1)	54.20(11)
Se(2)–Os(3)–Os(1)	55.59(8)
Os(2)–Os(3)–Os(1)	84.44(6)

4. Conclusions

The unsaturated cluster **2** is clearly a versatile reagent for the synthesis of open triangular *nido*-cluster **3**, the *closo*-triangular cluster **4** and the cubane-like cage cluster **5**. In contrast, the reaction of **1** with elemental selenium at 110 °C affords only intractable material. When treated with Me_3NO at 80 °C, compound **3** undergoes a self-condensation and forms the green dimer **7**. The formation of the dimer can be viewed as a back-to-back coupling of two $[Os_3(CO)_6(\mu_3\text{-}Se)_2(\mu\text{-}dppm)]$ units derived from **3** by loss of one CO-ligand. The two triosmium units are then joined through the

formation of three new osmium–osmium bonds. Compound **7** reacts with CO by cleavage of the three unsupported metal–metal bonds to regenerate **3** in high yield. Compound **3** reacts with PPh_3 in the presence of Me_3NO to afford the substitution product **8** along with the hexanuclear cluster **7**. The substitution of a carbonyl with PPh_3 does not cause significant structural alterations to the cluster framework, with all the important distances remaining effectively unchanged with respect to **3**. The reactions of dppmSe and $dppmSe_2$ with $[Os_3(CO)_{10}(MeCN)]$ provides a simple one-step synthetic procedure for the dppm-substituted selenido clusters **3**, **4**, **5** and **6** by oxidative addition and transfer of selenium atoms to the low-valent osmium centers. We anticipate further advances will be made in this area of research.

5. Supplementary material

Crystallographic data for the structural analyses have been deposited with the Cambridge Crystallographic Data Centre, CCDC Nos. 201321 for compound **3**, 201322 for compound **4**, 201323 for compound **6**, 201324 for compound **7**, and 201325 for compound **8**. Copies of this information may be obtained free of charge from The Director, CCDC, 12 Union Road Cambridge, CB2 1EZ, UK (Fax: +44-1223-336033; e-mail:deposit@ccdc.cam.ac.uk or www: http://www.ccdc.cam.ac.uk).

Acknowledgements

We gratefully acknowledge the Ministry of Science and Technology, Government of the Peoples' Republic of Bangladesh for financial assistance. KMAM acknowledges the EPSRC for the X-ray service at Cardiff.

References

[1] (a) M.I. Steigerwald, Polyhedron 13 (1994) 1245;
(b) G. Longoni, M.C. Iapalucci, In Clusters and Colloids, VCH, Weiheim, 1994, p. 132;
(c) L.C. Roof, J.W. Kolis, Chem. Rev. 93 (1993) 1037;
(d) J.G. Brennan, T. Siegrist, P.J. Carrol, S.M. Stuczynski, L.E. Brus, M.L. Steigerwald, J. Am. Chem. Soc. 111 (1989) 4141;
(e) Z. Nomikou, B. Schubert, R. Hoffmann, M.L. Steigerwald, Inorg. Chem. 31 (1992) 2201;
(f) D. Fenske, J. Ohmer, J. Hachgenci, Angew. Chem. Int. Ed. Engl. 24 (1985) 993;
(g) D. Fenske, H. Krautscheid, M. Muller, Angew. Chem. Int. Ed. Engl. 31 (1992) 321;
(h) D. Fenske, in: G. Schmid (Ed.), In Clusters and Colloids, VCH, Weinheim, 1994, p. 212.

[2] (a) R.D. Adams, Polyhedron 4 (1985) 2003;
(b) R.D. Adams, J.E. Babin, J.G. Wang, Polyhedron 8 (1989) 2351;
(c) Y. Mizobe, M. Hosomizu, J. Kawabato, M. Hidai, J. Chem. Soc. Chem. Commun. (1991) 1226.;
(d) R.D. Adams, J.E. Babin, P. Mathur, K. Natarajan, J.W. Wang, Inorg. Chem. 26 (1989) 1440;
(e) R.D. Adams, J.E. Babin, J. Estrada, J.-G. Wang, M.B. Hall, A.A. Low, Polyhedron 8 (1989) 1885.

[3] (a) T.M. Layer, J. Lewis, A. Martin, P.R. Raithby, W.-T. Wong, J. Chem. Soc. Dalton Trans. (1992) 3411.;
(b) P. Mathur, B.H.S. Thimmappa, A.L. Rheingold, Inorg. Chem. 29 (1990) 4658.

[4] (a) R.D. Adams, L.-W. Yang, J. Am. Chem. Soc. 104 (1982) 4115;
(b) R.D. Adams, I.T. Horvath, B.E. Segmuller, L.-W. Yang, Organometallics 2 (1983) 144, 1301.;
(c) R.D. Adams, G. Chen, S. Sun, T.A. Wolfe, J. Am. Chem. Soc. 112 (1990) 868;
(d) B.F.G. Johnson, J. Lewis, P.G. Lodge, P.R. Raithby, Acta Crystallogr. B 37 (1981) 1731;
(e) R.D. Adams, I.T. Horvath, Inorg. Chem. 23 (1984) 4718;
(f) P. Mathur, D. Chakrabarty, J. Organomet. Chem. 373 (1989) 129;
(g) P. Mathur, I.J. Mavunkal, V. Rugmini, Inorg. Chem. 28 (1989) 3616;
(h) P. Mathur, Adv. Organomet. Chem. 41 (1997) 243.

[5] (a) G. Hogarth, N.J. Taylor, A.J. Carty, A. Meyer, J. Chem. Soc. Chem. Commun. (1988) 834.;
(b) S.M. Stuczynski, Y.-U. Kwon, M.L. Steigerwald, J. Organomet. Chem. 449 (1993) 167;
(c) W. Imhof, G. Huttner, J. Organomet. Chem. 448 (1993) 247.

[6] (a) P. Baistrocchi, D. Cauzzi, M. Lanfranchi, G. Predieri, A. Tiripicchio, M.T. Camellini, Inorg. Chim. Acta 235 (1995) 173;
(b) P. Baistrocchi, M. Carezi, D. Cauzzi, C. Graiff, M. Lanfranchi, P. Manini, G. Predieri, A. Tiripicchio, Inorg. Chim. Acta 252 (1996) 367.

[7] (a) D. Cauzzi, C. Graiff, M. Lanfranchi, G. Predieri, A. Tiripicchio, J. Chem. Soc. Dalton Trans. (1995) 2321.;
(b) D. Cauzzi, C. Graiff, M. Lanfranchi, G. Predieri, A. Tiripicchio, J. Organomet. Chem. 536–537 (1997) 497;
(c) D. Cauzzi, C. Graiff, G. Predieri, A. Tiripicchio, C. Vignali, J. Chem. Soc. Dalton Trans. (1999) 237.;
(d) D. Cauzzi, C. Graiff, C. Massera, G. Predieri, A. Tiripicchio, D. Acquotti, J. Chem. Soc. Dalton Trans. (1999) 3515.

[8] (a) J.A. Akter, K.A. Azam, S.E. Kabir, K.M.A. Malik, Md.A. Mottalib, Inorg. Chem. Commun. 3 (2000) 553;
(b) A.J. Deeming, S.E. Kabir, J. Organomet. Chem. 340 (1988) 359;
(c) S.E. Kabir, A. Miah, L. Nesa, K. Uddin, K.I. Hardcastle, E. Rosenberg, A.J. Deeming, J. Organomet. Chem. 492 (1995) 41;
(d) S.R. Hodge, B.F.G. Johnson, J. Lewis, P.R. Raithby, J. Chem. Soc. Dalton Trans. (1987) 931.;
(e) B.F.G. Johnson, J. Lewis, M. Manari, D. Braga, F. Grepioni, C. Gradella, J. Chem. Soc. Dalton Trans. (1990) 2863.;
(f) D.F. Foster, J.H. Harrison, B.S. Nicholls, A.K. Smith, J. Organomet. Chem. 295 (1985) 99;
(g) K.-L. Lu, H.J. Chen, P.-Y. Lu, S.-Y. Li, S.-M. Hong, S.-M. Peng, G.-H. Lee, Organometallics 13 (1994) 585;
(h) S. Cartwright, J.A. Clucas, R.H. Dawson, D.F. Foster, M.M. Harding, A.K. Smith, J. Organomet. Chem. 302 (1986) 403.

[9] J.A. Clucas, D.F. Foster, M.M. Harding, A.K. Smith, J. Chem. Soc. Chem. Commun. (1984) 949.

[10] J.A. Clucas, M.M. Harding, A.K. Smith, J. Chem. Soc. Chem. Commun. (1985) 2080.

[11] M.P. Brown, P.A. Dolby, M.M. Harding, A.J. Mathews, A.K. Smith, J. Chem. Soc. Dalton Trans. (1993) 1671.

[12] K.A. Azam, M.B. Hursthouse, Md.R. Islam, S.E. Kabir, K.M.A. Malik, R. Miah, C. Sudbrake, H. Vahrenkamp, J. Chem. Soc. Dalton Trans. (1998) 1097.

[13] (a) J.A. Clucas, P.A. Dolby, M.M. Harding, A.K. Smith, J. Chem. Soc. Chem. Commun. (1987) 1829.;
(b) M.P. Brown, P.A. Dolby, M.M. Harding, A.J. Mathews, A.K. Smith, D. Osella, M. Arbrun, R. Gobetto, P.R. Raithby, P. Zanello, J. Chem. Soc. Dalton Trans. (1993) 827.
[14] M.M. Harding, B. Kariuki, A.J. Mathews, A.K. Smith, P. Braunstein, J. Chem. Soc. Dalton Trans. (1994) 33.
[15] R.A. Bartlett, C.J. Cardin, D.J. Cardin, G.A. Lawless, M.J. Power, P.P. Power, J. Chem. Soc. Chem. Commun. (1988) 312.
[16] S.M.T. Abedin, K.A. Azam, M.B. Hursthouse, S.E. Kabir, K.M.A. Malik, Md.A. Mottalib, E. Rosenberg, J. Cluster Sci. 12 (2001) 5.
[17] S.E. Kabir, K.M.A. Malik, E. Mollah, Md.A. Mottalib, J. Organomet. Chem. 616 (2000) 157.
[18] S.E. Kabir, C.A. Johns, K.M.A. Malik, Md.A. Mottalib, E. Rosenberg, J. Organomet. Chem. 625 (2001) 112.
[19] S.M.T. Abedin, K.I. Hardcastle, S.E. Kabir, K.M.A. Malik, Md.A. Mottalib, E. Rosenberg, M.J. Abedin, Organometallics 19 (2000) 5623.
[20] K.A. Azam, G.M.G. Hossain, S.E. Kabir, K.M.A. Malik, Md.A. Mottalib, S. Pervin, N.C. Sarker, Polyhedron 21 (2002) 381.
[21] (a) B.F.G. Johnson, J. Lewis, D.A. Pippard, J. Chem. Soc. Dalton Trans. (1981) 407.;
(b) J.N. Nicholls, M.D. Vargas, Inorg. Synth. 26 (1989) 289.
[22] (a) A.M. Bond, R. Cotton, P. Panagiotidou, Organometallics 7 (1988) 1767;
(b) S.O. Grim, E.D. Walton, Inorg. Chem. 19 (1980) 1982.
[23] R. Hooft, COLLECT Data Collection Software, Nonius B.V., Delft, The Netherlands, 1998.
[24] Z Otwinowski, W. Minor, in: C.W. Carter, Jr., R.M. Sweet (Eds.), In Macromolecular Crystallography, Academic Press, New York, 1997, pp. 307–326.
[25] R.H. Blessing, Acta Crystallogr. A 51 (1995) 33.
[26] R.H. Blessing, J. Appl. Crystallogr. A 51 (1995) 33.
[27] G.M. Sheldrick, Acta Crystallogr. A 46 (1990) 467.
[28] G.M. Sheldrick, SHELXL-97, Program for Crystal Structure Refinement, University of Göttingen, Germany, 1997.
[29] XSCANS Data Collection Software, Release 2.10b. Bruker AXS, Inc., Madison, WI, 1994.
[30] L.J. Farrugia, J. Appl. Crystallogr. 32 (1999) 837.
[31] M.R. Churchill, B.G. DeBoer, Inorg. Chem. 16 (1977) 878.
[32] R.D. Adams, I.T. Horvath, H.-S. Kim, Organometallics 3 (1984) 548.
[33] B.F.G. Johnson, J. Lewis, P.G. Lodge, P.R. Raithby, Acta Crystallogr. B 37 (1981) 1731.
[34] D.J. Dahm, R.A. Jacobson, J. Am. Chem. Soc. 90 (1968) 5106.
[35] E.J. Forbes, N. Goodhand, D.L. Jones, T.A. Hamor, J. Organomet. Chem. 182 (1979) 143.
[36] R.E. Benfield, B.F.G Johnson, G.M. Sheldrick, Acta Crystallogr. B 34 (1978) 666.
[37] S.E. Kabir, K.M.A. Malik, M.A. Mottalib, J. Chem. Crystallogr. 29 (1999) 7.
[38] (a) A.J. Arce, P. Arrojo, Y.De. Sanctis, A.J. Deeming, D.J. West, Polyhedron 11 (1992) 1013;
(b) B.F.G. Johnson, J. Lewis, P.G. Lodge, P.R. Raithby, K. Henrick, M. McPartlin, J. Chem. Soc. Chem. Commun. (1979) 719.
[39] (a) P. Mathur, I.J. Mavunkal, J. Organomet. Chem. 350 (1988) 251;
(b) P. Mathur, I.J. Mavunkal, V. Rugmini, J. Organomet. Chem. 367 (1989) 243.
[40] R.D. Adams, I.T. Horvath, J. Am. Chem. Soc. 106 (1984) 1869.